CrossMark

ORIGINAL ARTICLE

Redox potentials of ubiquinone, menaquinone, phylloquinone, and plastoquinone in aqueous solution

Shinnosuke Kishi[1] · Keisuke Saito[1,2] · Yuki Kato[3] · Hiroshi Ishikita[1,2]

Abstract Quinones serve as redox active cofactors in bacterial photosynthetic reaction centers: photosystem I, photosystem II, cytochrome bc_1, and cytochrome b_6f. In particular, ubiquinone is ubiquitous in animals and most bacteria and plays a key role in several cellular processes, e.g., mitochondrial electron transport. Their experimentally measured redox potential values for one-electron reduction $E_m(Q/Q^{\cdot-})$ were already reported in dimethylformamide (DMF) versus saturated calomel electrode but not in water versus normal hydrogen electrode (NHE). We calculated $E_m(Q/Q^{\cdot-})$ of 1,4-quinones using a quantum chemical approach. The calculated energy differences of reduction of Q to $Q^{\cdot-}$ in DMF and water for 1,4-quinone derivatives correlated highly with the experimentally measured $E_m(Q/Q^{\cdot-})$ in DMF and water, respectively. $E_m(Q/Q^{\cdot-})$ were calculated to be −163 mV for ubiquinone, −260 mV for menaquinone and phylloquinone, and −154 mV for plastoquinone in water versus NHE.

✉ Hiroshi Ishikita
hiro@appchem.t.u-tokyo.ac.jp

[1] Department of Applied Chemistry, The University of Tokyo, 7-3-1 Hongo, Bunkyo-ku, Tokyo 113-8654, Japan

[2] Research Center for Advanced Science and Technology, The University of Tokyo, 4-6-1 Komaba, Meguro-ku, Tokyo 153-8904, Japan

[3] Division of Material Science, Graduate School of Science, Nagoya University, Furo-cho, Chikusa-ku, Nagoya 464-8602, Japan

Introduction

Quinones can accept two electrons and two protons via the initial protonation of semiquinone ($Q^{\cdot-}$ to $QH^{\cdot}$) and the second protonation of hydroquinone (QH^- to QH_2). Ubiquinone serves as an electron acceptor at the Q_A and Q_B binding sites in reaction centers of purple bacteria (PbRC) from *Rhodobacter sphaeroides* and serves as an electron donor in cytochrome bc_1. Similarly, menaquinone (vitamin K_2) is the acceptor at the Q_A site in PbRC from *Blastochloris viridis*, whereas phylloquinone (vitamin K_1) is the active center at the A_{1A} and A_{1B} sites in photosystem I (PSI). In reaction centers of green non-sulfur bacteria from *Chloroflexus aurantiacus*, menaquinones are also located at both Q_A and Q_B sites (Hale et al. 1983). It should be noted that phylloquinone and menaquinone have the same head-group structure (Fig. 2). Plastoquinone serves as an electron acceptor at the Q_A and Q_B sites in photosystem II (PSII) (Fig. 1) (Robinson and Crofts 1984; Rutherford et al. 1984; Okamura et al. 2000; Brettel and Leibl 2001; Wraight 2004) and serves as an electron donor in cytochrome b_6f. In PbRC and PSII, both Q_A and Q_B are located near the non-heme Fe^{2+}, and the Fe^{2+} ligands (i.e., His-L190 and His-M217 (or M219) in PbRC and D1-His215 and D2-His214 in PSII) donate an H-bond to the carbonyl O atoms of quinones that are proximal to the Fe complex (O_{prox}) (Fig. 1a–c). The carbonyl O atoms of quinones at the distal position (O_{dist}) also form H-bonds with the proteins. On the other hand, the non-heme Fe^{2+} is absent in PSI, but the Fe_4S_4 cluster F_X is located near the two A_1 binding sites (Fig. 1d).

Redox potential values for one-electron reduction, $E_m(Q/Q^{\cdot-})$, for 1,4-quinones, including ubiquinone, menaquinone (phylloquinone), and plastoquinone, were experimentally measured in dimethylformamide (DMF) versus saturated calomel electrode (SCE) by Prince et al.

(a) PbRC (*Blc. viridis*)

(b) PbRC (*Rb. sphaeroides*)

(c) PSII

(d) PSI

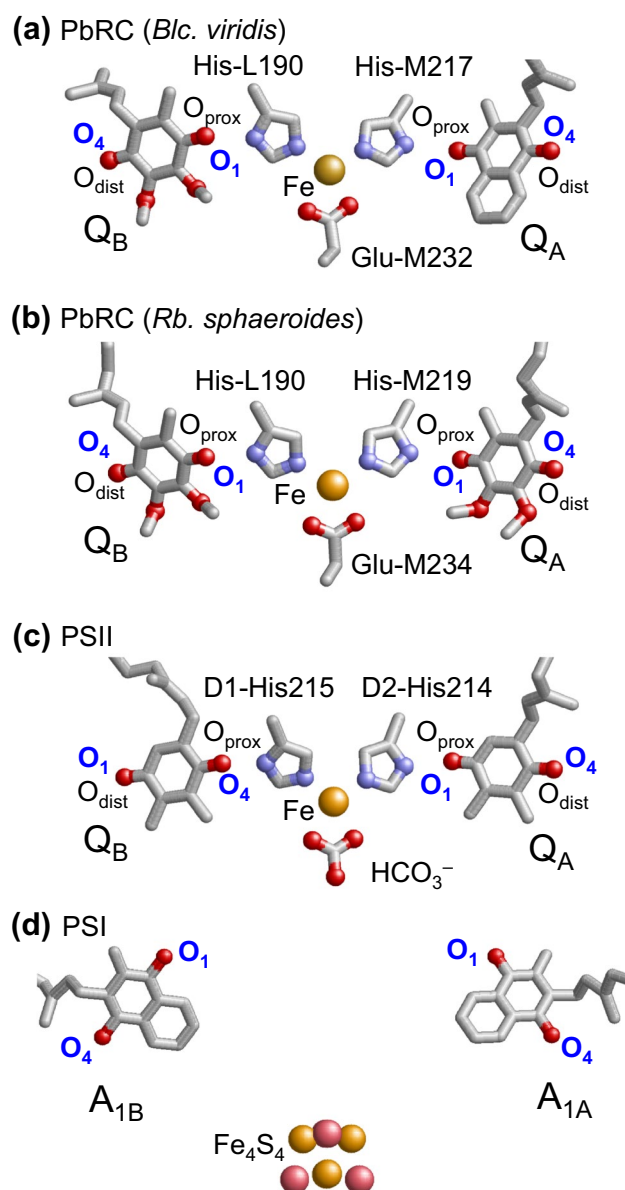**Fig. 1** Quinones in photosynthetic reaction centers: **a** menaquinone as Q_A and ubiquinone as Q_B in bacterial photosynthetic reaction centers from *Blastochloris viridis* (*Blc. viridis*, PDB ID: 2I5N) (Li et al. 2006), **b** ubiquinone as Q_A and Q_B in bacterial photosynthetic reaction centers from *Rhodobacter sphaeroides* (*Rb. sphaeroides*, PDB ID: 3I4D), **c** plastoquinone as Q_A and Q_B in PSII (PDB ID: 3ARC) (Umena et al. 2011), and **d** phylloquinone as A_{1A} and A_{1B} in PSI (PDB ID: 1JB0) (Jordan et al. 2001). *Red* and *blue balls* indicate O and N atoms, respectively. In PbRC and PSII, O_{prox} and O_{dist} stand for O atoms of the quinones at the proximal and distal positions with respect to the non-heme Fe complex, respectively. Note that except for Q_B in PSII, O_{prox} is O1 and O_{dist} is O4 in PbRC and PSII

Fig. 2 Molecular structures of **a** ubiquinone ($n = 10$), **b** menaquinone and phylloquinone ($n = 3$ to 9), and **c** plastoquinone ($n = 6$ to 9), where n is the number of isoprene units

(Prince et al. 1983). $E_m(Q/Q^{·-})$ for 1,4-quinones were also experimentally measured in water versus normal hydrogen electrode (NHE) by Swallow (1982). Since E_m
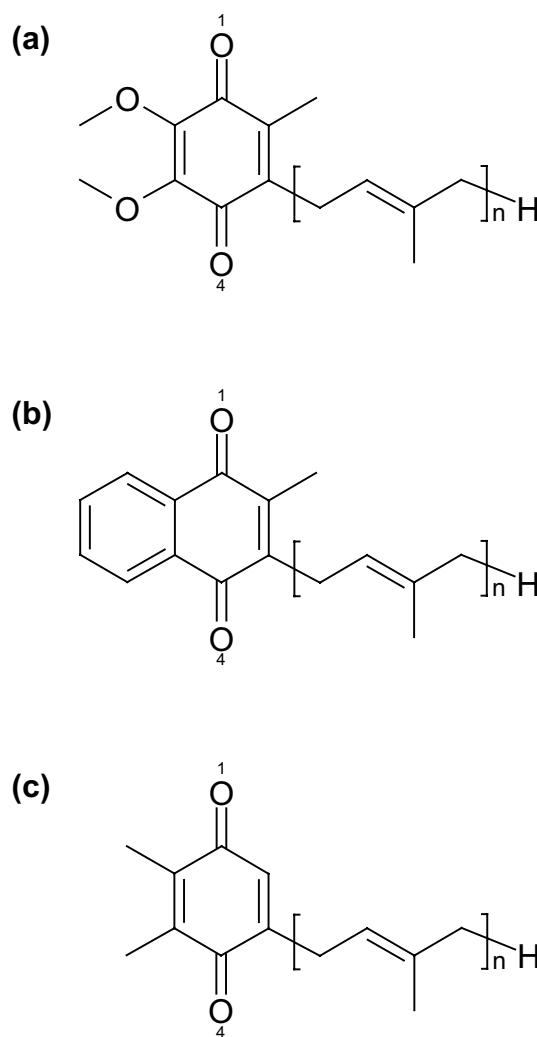
values for redox active sites in proteins are often reported as the values measured in water versus NHE, $E_m(Q/Q^{·-})$ for ubiquinone, menaquinone (phylloquinone), and plastoquinone measured in water versus NHE are preferentially required when analyzing interaction between the quinone binding site and the protein environment in PbRC, PSI, PSII, cytochrome bc_1, and cytochrome b_6f. However, as far as we are aware, experimentally measured $E_m(Q/Q^{·-})$ for ubiquinone, menaquinone (phylloquinone), and plastoquinone in water versus NHE have not been reported (Fig. 2). Here, we report $E_m(Q/Q^{·-})$ for ubiquinone, menaquinone (phylloquinone), and plastoquinone in water versus NHE, obtained using a quantum chemical approach.

Computational procedures

In reduction of the oxidized state (A) to reduced state (A$^{\cdot-}$) in aqueous solution, the redox potential E_m relative to the normal hydrogen electrode (NHE) is defined as

$$E_m = -\frac{\Delta G_{aq}}{nF}, \tag{1}$$

where ΔG_{aq} is the free energy difference between A and A$^{\cdot-}$ [i.e., $\Delta G_{aq} = G_{aq}(A^{\cdot-}) - G_{aq}(A) - G_{NHE}$], n is the number of electron involved in the reaction (i.e., $n = 1$ in the present case), and F is the Faraday constant. ΔG_{aq} can also be approximated as

$$\Delta G_{aq} = k\Delta E_{QM/PCM} + C, \tag{2}$$

where k is the scaling factor, $\Delta E_{QM/PCM}$ is the energy difference between A and A$^{\cdot-}$ in aqueous phase [i.e., $\Delta E_{QM/PCM} = E_{QM/PCM}(A^{\cdot-}) - E_{QM/PCM}(A)$], which can be calculated using a quantum chemical approach with the polarizable continuum model (PCM) method, and C is a constant (Matsui et al. 2012; Hasegawa et al. 2017). The Eq. 1 can be written as Eq. 3 using Eq. 2,

$$E_m = k'\Delta E_{QM/PCM} + C', \tag{3}$$

where k' is the scaling factor and C' is a constant (Matsui et al. 2012; Hasegawa et al. 2017). To determine k' and C', we calculated $\Delta E_{QM/PCM(DMF)}$ (and $\Delta E_{QM/PCM(water)}$) for ten (nine) 1,4-quinones whose experimentally measured $E_m(Q/Q^{\cdot-})$ are reported for DMF (Prince et al. 1983) [and water (Swallow 1982)].

We employed the unrestricted density functional theory (DFT) method with the B3LYP functional and 6-31g++** basis sets for Q$^{\cdot-}$ (the total spin $S = 1/2$) and the restricted DFT method for Q ($S = 0$), using the Gaussian (Frisch et al. 2004) program code with the PCM method. Solvent molecules were considered implicitly, using the SCRF = water option and the SCRF = Dimethylformamide option with the values of 78.3553 for water and 37.219 for DMF for dielectric constant (i.e., default values), respectively. However, it should be noted that it is only one of many internal parameters used to define solvents in the PCM method (Frisch et al. 2004). Thus, simply changing the dielectric constant value will not define a new solvent properly.

Since the isoprene units do not comprised conjugated double bonds, the isoprene side-chain length n (Fig. 2) was set to 1 or 2 for the calculations of ubiquinone, menaquinone (phylloquinone), and plastoquinone similar to previous studies (Hasegawa et al. 2017). This could also reduce the number of possible conformations. In fact, the length of the ubiquinone does not practically affect its energetics, as demonstrated by the similar experimentally measured $E_m(Q/Q^{\cdot-})$ values of ubiquinone-1 and -10 in DMF (−611 and −602 mV versus SCE, respectively) (Prince et al. 1983). It should also

be noted that $n = 0$, which corresponds to 2,3-dimethoxy-5-methyl-1,4-benzoquinone [$E_m(Q/Q^{\cdot-}) = -539$ mV in DMF versus SCE (Prince et al. 1983)], i.e., ubiquinone-0, as presented in Ref. (Cape et al. 2006), is a less relevant representation of $E_m(Q/Q^{\cdot-})$ for quinones in PbRC, PSI, PSII, cytochrome bc_1, and cytochrome b_6f. Ubiquinone-0 corresponds to 2,3-dimethoxy-5-methyl-1,4-benzoquinone rather than 2,3-dimethoxy-5,6-dimethyl-1,4-benzoquinone [in contrast to the statement in ref. (Prince et al. 1983)].

Results and discussion

Correlation of calculated energies with experimentally measured $E_m(Q/Q^{\cdot-})$ for 1,4-quinones in DMF and water

The calculated $\Delta E_{QM/PCM}$ for reduction of deprotonated Q to Q$^{\cdot-}$ for ten 1,4-quinones in DMF ($\Delta E_{QM/PCM(DMF)}$) and water ($\Delta E_{QM/PCM(water)}$) were highly associated with the experimentally measured $E_m(Q/Q^{\cdot-})$ in DMF, ranging from −401 to −751 mV versus SCE (Prince et al. 1983), and the experimentally measured $E_m(Q/Q^{\cdot-})$ in water, ranging from −240 to 99 mV versus NHE (Swallow 1982), which were best fitted to the following equations (Figs. 3a, b):

$$E_m(Q/Q^{\cdot-}) \text{ in DMF versus SCE [mV]}$$
$$= -32.1 \left(\Delta E_{QM/PCM(DMF)} + 108.54 \, [\text{kcal/mol}]\right) \tag{4}$$

$$E_m(Q/Q^{\cdot-}) \text{ in water versus NHE [mV]}$$
$$= -33.3 \left(\Delta E_{QM/PCM(water)} + 93.95 \, [\text{kcal/mol}]\right). \tag{5}$$

Using Eqs. 4 and 5, the calculated $E_m(Q/Q^{\cdot-})$ in DMF versus SCE and $E_m(Q/Q^{\cdot-})$ in water versus NHE for ten and nine 1,4-quinones, respectively, are listed in Table 1. Our results confirm that Eqs. 4 and 5 can reproduce the experimentally measured $E_m(Q/Q^{\cdot-})$ in DMF versus SCE and $E_m(Q/Q^{\cdot-})$ in water versus NHE, respectively. The overall root mean square deviation between the experimentally measured $E_m(Q/Q^{\cdot-})$ in DMF versus SCE and the calculated $E_m(Q/Q^{\cdot-})$ in DMF versus SCE based on Eq. 4 for the ten 1,4-quinones is ±21 mV. The overall root mean square deviation between the experimentally measured $E_m(Q/Q^{\cdot-})$ in water versus NHE and the calculated $E_m(Q/Q^{\cdot-})$ in water versus NHE based on Eq. 5 for the nine 1,4-quinones is ±16 mV. These deviations are sufficiently small with respect to those obtained in other theoretical studies [e.g., ±131 mV (Schmidt am Busch and Knapp 2005)].

Notably, to obtain Eq. 4, $E_m(Q/Q^{\cdot-})$ for ubiquinone, menaquinone (phylloquinone), and plastoquinone in DMF versus SCE were not included [where $k = -32.1$ (mV mol/kcal), $C = -108.5$ (mV), excluding ubiquinone, menaquinone (phylloquinone), and plastoquinone]. Nevertheless,

the experimentally measured $E_m(Q/Q^{\cdot-})$ in DMF versus
SCE (Prince et al. 1983) and the calculated $\Delta E_{QM/PCM(DMF)}$
for ubiquinone, menaquinone (phylloquinone), and plasto-
quinone can also be described by Eq. 4 [where $k = -31.8$
(mV mol/kcal), $C = -108.8$ (mV), including ubiqui-
none, menaquinone (phylloquinone), and plastoquinone]
(Fig. 3a), which demonstrates that $E_m(Q/Q^{\cdot-})$ for ubiqui-
none, menaquinone (phylloquinone), and plastoquinone can
be described accurately by Eqs. 4 and 5.

In contrast to other quantum chemical approaches, e.g.,
(Schmidt am Busch and Knapp 2005), the present approach
neither need to calculate the zero-point vibrational energy
and the excess vibrational free energy at 298 K for both
Q and $Q^{\cdot-}$ nor optimize the atomic radii of $Q/Q^{\cdot-}$ for the
solvation energy. Once k' and C' are uniquely determined,
$E_m(Q/Q^{\cdot-})$ can be accurately calculated based on calcu-
lated $\Delta E_{QM/PCM}$, without considering further details of
$Q/Q^{\cdot-}$ and solvent. The strong correlation between experi-
mentally measured $E_m(Q/Q^{\cdot-})$ and calculated $\Delta E_{QM/PCM}$
(Fig. 3), in turn, suggests that k' and C' are similar for these
1,4-quinones.

In the present study, solvent molecules were considered
implicitly. This treatment is more appropriate to describe
H-bonds between quinones and bulk water/solvent mol-
ecules, in which the H-bond patterns are not unique, e.g.,
bulk solvent. Explicit water/solvent models may be able to
describe H-bonds adequately when the H-bond pattern is
unique [e.g., water molecules in the well-ordered cluster
near the Mn_4CaO_5 cluster (Saito et al. 2011; Sakashita et al.
2017)] or all possible (H-bond) conformations of water/
solvent molecules can be evaluated, e.g., using molecular
dynamics simulations; this is not the case for 1,4-quinones
investigated in the present study.

We found that the experimentally measured $E_m(Q/Q^{\cdot-})$ for
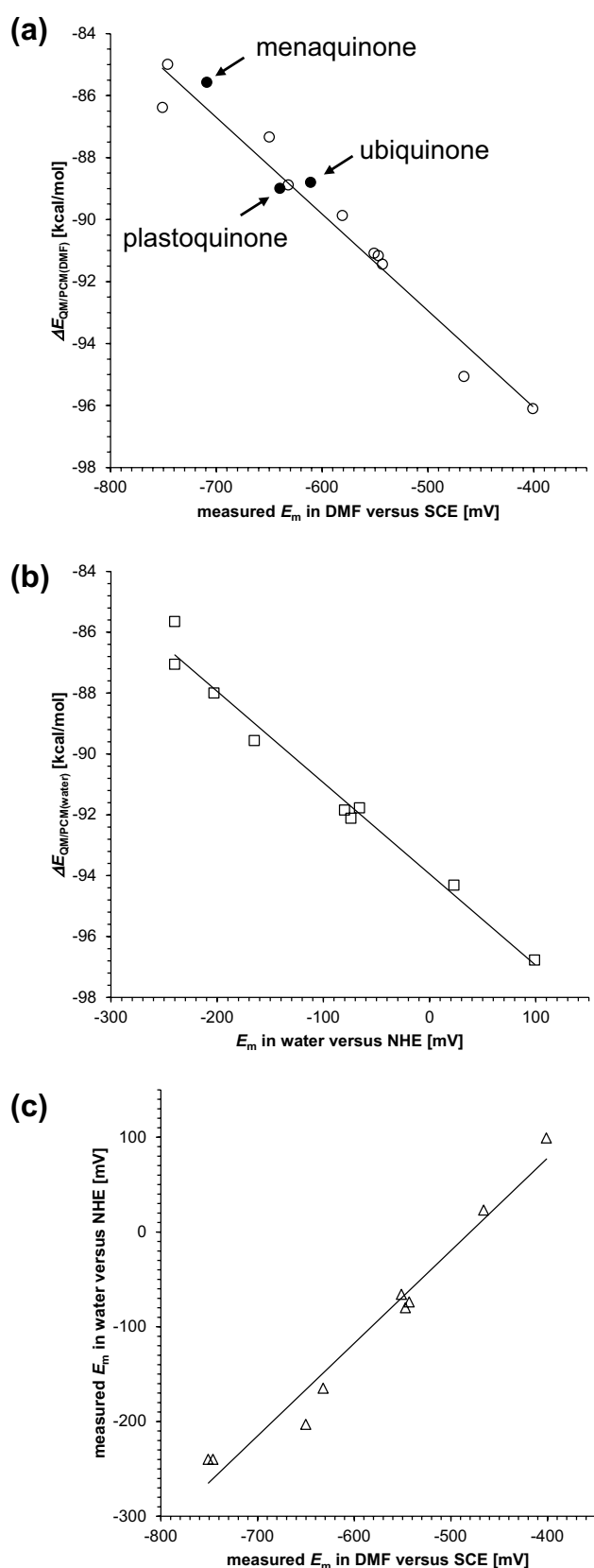the nine 1,4-quinones in water versus NHE (Swallow 1982)

Table 1 Experimentally measured $E_m(Q/Q^{·-})$ (exp.) versus SCE (Prince et al. 1983; Swallow 1982) and calculated $E_m(Q/Q^{·-})$ (calc.) versus NHE

	E_m in DMF (vs. SCE)		E_m in water[a] (vs. NHE)	
	exp.[b]	calc.	exp.[c]	calc.
1,4-Benzoquinone	−401	−399	99	94
Methyl-1,4-benzoquinone	−466	−432	23	12
2,3-Dimethyl-1,4-benzoquinone	−543	−548	−74	−61
2,5-Dimethyl-1,4-benzoquinone	−551	−559	−66	−72
2,6-Dimethyl-1,4-benzoquinone	−547	−557	−80	−70
Trimethyl-1,4-benzoquinone	−632	−630	−165	−146
Tetramethyl-1,4-benzoquinone [d]	−751	−710	−240	−230
1,4-Naphtoquinone	−581	−598	n.d.	−114
2-Methyl-1,4-naphtoquinone	−650	−679	−203	−198
2,3-Dimethyl-1,4-naphtoquinone	−746	−755	−240	−276
Ubiquinone-1	−611	−633	n.d.	−163
Menaquinone-1 (phylloquinone-1)	n.d.	−738	n.d.	−260
Menaquinone-2	−709	−736	n.d.	−256
Plastoquinone-1	−640	−626	n.d.	−154

n.d. Not determined

[a] pH 7

[b] Ref. (Prince et al. 1983)

[c] Ref. (Swallow 1982)

[d] Duroquinone

and DMF versus SCE (Prince et al. 1983) correlated strongly (Fig. 3c), which were best fitted to the following equation:

$$E_m(Q/Q^{·-}) \text{ in water versus NHE [mV]}$$
$$= 0.98 \, [E_m(Q/Q^{·-}) \text{ in DMF versus SCE } + 480]. \quad (6)$$

Equation 6 indicates that experimentally measured $E_m(Q/Q^{·-})$ in DMF versus SCE can be practically converted to $E_m(Q/Q^{·-})$ in water versus NHE by adding 480 mV. The E_m difference of 480 mV may also contain a liquid junction potential between SCE in DMF and NHE in water. The liquid junction potential can be ignored when $E_m(Q/Q^{·-})$ are compared versus ferrocene (Fc/Fc⁺); e.g., $E_m(Q/Q^{·-})$ for 1,4-benzoquinone is experimentally measured to be −401 mV in DMF versus SCE, where $E_m(Fc/Fc^+) = 524$ mV (Prince et al. 1983). Since $E_m(Fc/Fc^+) = 400$ mV in water versus NHE (Koepp et al. 1960), $E_m(Q/Q^{·-})$ for 1,4-benzoquinone is −925 mV in DMF versus Fc/Fc⁺ and 301 mV in water versus Fc/Fc⁺, which indicates that $E_m(Q/Q^{·-})$ for 1,4-benzoquinone in DMF and water originally differ by 624 mV in the absence of the liquid junction potential (Table 2). This holds true for all 1,4-quinones investigated. It seems likely that $E_m(Q/Q^{·-})$ for 1,4-benzoquinones already differ by 600 mV even in the absence of the liquid junction potential (Table 2). The presence of H-bond donor to Q^{·-} in water is partly responsible for the E_m difference of 600 mV, since the presence of H-bond donor to Q^{·-} stabilizes Q^{·-} and increases $E_m(Q/Q^{·-})$. Nevertheless, the entire

Table 2 Experimentally measured $E_m(Q/Q^{·-})$ (exp.) (Prince et al. 1983; Swallow 1982), calculated $E_m(Q/Q^{·-})$ (calc.) versus ferrocene (Fc/Fc⁺), and the difference in $E_m(Q/Q^{·-})$ (ΔE_m)

	E_m in DMF (vs. Fc/Fc⁺)		E_m in water[a] (vs. Fc/Fc⁺)		ΔE_m (DMF–water)	
	exp.[b]	calc.	exp.[c]	calc.	exp.	calc.
1,4-Benzoquinone	−925	−923	−301	−306	−624	−617
Methyl-1,4-benzoquinone	−990	−956	−377	−388	−613	−568
2,3-Dimethyl-1,4-benzoquinone	−1067	−1072	−474	−461	−593	−611
2,5-Dimethyl-1,4-benzoquinone	−1075	−1083	−466	−472	−609	−611
2,6-Dimethyl-1,4-benzoquinone	−1071	−1081	−480	−470	−591	−611
Trimethyl-1,4-benzoquinone	−1156	−1154	−565	−546	−591	−608
Tetramethyl-1,4-benzoquinone[d]	−1275	−1234	−640	−630	−635	−604
1,4-Naphtoquinone	−1105	−1122	n.d.	−400	n.d.	n.d.
2-Methyl-1,4-naphtoquinone	−1174	−1203	−603	−598	−571	−605
2,3-Dimethyl-1,4-naphtoquinone	−1270	−1279	−640	−676	−630	−602
Ubiquinone-1	−1135	−1157	n.d.	−563	n.d.	−593
Menaquinone-2 (phylloquinone-2)	−1233	−1260	n.d.	−660	n.d.	−600
Plastoquinone-1	−1164	−1150	n.d.	−554	n.d.	−596

n.d. Not determined

[a] pH 7

[b] Ref. (Prince et al. 1983)

[c] Ref. (Swallow 1982)

[d] Duroquinone

difference of 600 mV would not be explained solely by the first sphere water molecules that can directly form an H-bond with Q$^{\cdot-}$. The surrounding water molecules (e.g., second and third sphere molecules) cannot directly form an H-bond with Q$^{\cdot-}$ but the Q$^{\cdot-}$ stabilization is pronounced by their dipole orientations (Takaoka et al. 2016). The corresponding effect may be ignored in DMF with respect to water.

As far as only E_m differences among the redox active cofactors (ΔE_m) are discussed in the same proteins, e.g., along the electron transfer chains, E_m values of isolated cofactors measured in DMF, which are reported also for chlorophylls (Watanabe and Kobayashi 1991), might possibly be useful. On the other hand, when E_m values in the protein environments are discussed, comparison with E_m values of isolated cofactors measured in water is recommended, since E_m values measured in DMF is originally 600 mV lower than those measured in water even in the absence of the liquid junction potential (Table 2).

$E_m(Q/Q^{\cdot-})$ for ubiquinone, menaquinone, phylloquinone, and plastoquinone in water versus NHE

To the best of our knowledge, experimentally measured $E_m(Q/Q^{\cdot-})$ for ubiquinone, menaquinone (phylloquinone), and plastoquinone in water versus NHE are not reported. By calculating $\Delta E_{QM/PCM(water)}$ and using Eq. 5, $E_m(Q/Q^{\cdot-})$ was calculated to be −163 mV for ubiquinone, −260 mV for menaquinone (phylloquinone), and −154 mV for plastoquinone in water versus NHE (Table 1).

In ubiquinone, one of the 2,3-methoxy groups lies outside the quinone ring. Hence, Zhu and Gunner proposed that $E_m(Q/Q^{\cdot-})$ for ubiquinone, a 2,3-dimethoxy-5-methyl-6-isoprenyl benzoquinone, is more similar to the $E_m(Q/Q^{\cdot-})$ for trimethyl-benzoquinone than to the $E_m(Q/Q^{\cdot-})$ for tetramethyl-benzoquinone (Zhu and Gunner 2005). Indeed, the calculated $E_m(Q/Q^{\cdot-})$ = −163 mV for ubiquinone (Table 1) is close to the experimentally measured $E_m(Q/Q^{\cdot-})$ = −165 mV for trimethyl-benzoquinone (Swallow 1982) in water versus NHE, which is consistent with their proposal. Although it was proposed that difference in the 2-methoxy orientation of ubiquinone was responsible for the E_m difference of more than 160 mV between Q_A and Q_B in PbRC (Taguchi et al. 2013), the similar $E_m(Q/Q^{\cdot-})$ values of trimethyl-benzoquinone and ubiquinone (ref. (Zhu and Gunner 2005) and Table 1) suggest that contributions of methoxy and methyl groups to $E_m(Q/Q^{\cdot-})$ are not significantly different. It should also be noted that estimation by Swallow resulted in a more negative value of $E_m(Q/Q^{\cdot-})$ = −230 ± 20 mV for ubiquinone at pH 7 (Swallow 1982).

The present study shows that $E_m(Q/Q^{\cdot-})$ is −260 mV for menaquinone (phylloquinone) in water versus NHE (Table 1); the calculated $E_m(Q/Q^{\cdot-})$ can be confirmed

by Eq. 6, which can be reproduced by adding 480 mV to $E_m(Q/Q^{\cdot-})$ in DMF versus SCE. Previously, Ptushenko et al. considered that $E_m(Q/Q^{\cdot-})$ was −800 mV for phylloquinone in DMF versus NHE by considering a liquid junction potential between SCE in DMF and NHE in water (Ptushenko et al. 2008). Using the low $E_m(Q/Q^{\cdot-})$ value of −800 mV for phylloquinone in DMF versus NHE, they obtained $E_m(A_{1A})$ = −671 mV and $E_m(A_{1B})$ = −844 mV (Ptushenko et al. 2008), and were able to reproduce the reported low $E_m(A_1)$ in PSI [e.g., −810 mV (Vos and van Gorkom 1990), −754 mV (Iwaki and Itoh 1994), and lower than −700 mV (Brettel and Leibl 2001)]. This, in turn, suggests that the electrostatic interaction of the PSI protein environment at the A_1 site is remarkably weak in their computational model. If this is the case, then $E_m(Q_A)$ of −150 mV for the same quinone species (menaquinone) would be regarded as being "unusually high" in PbRC from *Blastochloris viridis* (Brettel and Leibl 2001), and the PbRC protein environment must dramatically increase $E_m(Q/Q^{\cdot-})$ for menaquinone by more than 600 mV at the Q_A site in their computational model; obviously this is not the case for the PbRC protein environment, as already demonstrated in theoretical studies (Rabenstein et al. 1998; Ishikita and Knapp 2004; Zhu and Gunner 2005). $E_m(Q/Q^{\cdot-})$ = −260 mV for menaquinone (phylloquinone) in water versus NHE (Table 1) suggests that the PSI protein environment (e.g., the presence of negatively charged F_X near A_1 (Ishikita and Knapp 2003)) is responsible for low $E_m(A_1)$ in PSI. When $E_m(Q/Q^{\cdot-})$ = −800 mV for phylloquinone in DMF versus NHE is used, the resulting $E_m(A_1)$ should contain the E_m downshift of ca. 600 mV with respect to water versus NHE as an artifact (Table 2), since the PSI is not solvated in DMF but in water in the thylakoid membrane. One can directly focus on the influence of the PSI protein environment on $E_m(A_1)$ when using $E_m(Q/Q^{\cdot-})$ = −260 mV in water versus NHE. It seems plausible that using E_m values measured in water is more recommended to analyze E_m values for the redox active groups in proteins unless the proteins are solvated in DMF.

This fact would be more obvious when considering E_m of heme proteins or flavin-binding proteins. E_m of heme (Harbury and Loach 1960; Wilson 1983) and flavin (Draper and Ingraham 1968; Anderson 1983) were experimentally measured in water. These cofactors are often largely exposed to the protein bulk surface [e.g., heme (Kerfeld et al. 2003; Clarke et al. 2011) and flavin-binding (Ludwig et al. 1997; Watt et al. 1991) proteins]. As these cofactors are released away from the binding site toward the bulk region, the E_m values must be close to those experimentally measured in water; this is exactly the case for Q_B in PbRC and PSII, which is located near the protein bulk surface. Using spectroelectrochemistry, Kato et al. directly determined $E_m(Q_B)$ to be +90 mV in PSII from *Thermosynechococcus elongates* versus NHE (Kato et al. 2016). $E_m(Q/Q^{\cdot-})$ is −154 mV for

plastoquinone in water versus NHE (Table 1) and would be -750 mV in DMF versus NHE (assuming E_m downshift of ca. 600 mV, Table 2). If $E_m(Q/Q^{\cdot-})$ measured in DMF were relevant, the PSII protein environment would need to increase $E_m(Q/Q^{\cdot-})$ for plastoquinone by 840 mV at the Q_B site. In addition, $E_m(Q_A)$ was determined to be -145 mV in spinach PSII versus NHE, using spectroelectrochemistry (Brinkert et al. 2016); the PSII protein environment would also need to increase $E_m(Q/Q^{\cdot-})$ for plastoquinone by 600 mV even at the Q_A site, which is less exposed to the protein bulk surface. It seems likely that E_m values for quinones measured in water are more recommended when comparing with $E_m(Q/Q^{\cdot-})$ in the protein environments. This would also hold true for the quinone binding sites in cytochrome bc_1 and cytochrome $b_6 f$, at which quinones from PbRC and PSII can bind, respectively.

Conclusion

Experimentally measured $E_m(Q/Q^{\cdot-})$ in DMF versus SCE (Prince et al. 1983) and $E_m(Q/Q^{\cdot-})$ in water versus NHE (Swallow 1982) correlated highly with the quantum chemically calculated energy differences ($\Delta E_{QM/PCM}$) between neutral and reduced states (Figs. 3a, b) and can be best fitted to Eqs. 4 and 5, respectively. It seems likely that $E_m(Q/Q^{\cdot-})$ for 1,4-benzoquinones differ by 600 mV even in the absence of the liquid junction potential between DMF and NHE (versus Fc/Fc^+). $E_m(Q/Q^{\cdot-})$ was calculated to be -163 mV for ubiquinone, -260 mV for menaquinone (phylloquinone), and -154 mV for plastoquinone in water versus NHE (Table 1). In particular, $E_m(Q/Q^{\cdot-}) = -260$ mV for phylloquinone in water versus NHE unambiguously demonstrates that remarkably low $E_m(A_1)$ in PSI does not originate from $E_m(Q/Q^{\cdot-})$ for phylloquinone but from interaction with the PSI protein environment, as suggested previously (Ishikita and Knapp 2003). These $E_m(Q/Q^{\cdot-})$ are prerequisite for analyzing the $E_m(Q/Q^{\cdot-})$ shift caused by electrostatic interactions within the protein environment in photosynthetic reaction centers.

References

Anderson RF (1983) Energetics of the one-electron reduction steps of riboflavin, FMN and FAD to their fully reduced forms. Biochim Biophys Acta 722:158–162

Brettel K, Leibl W (2001) Electron transfer in photosystem I. Biochim Biophys Acta 1507:100–114

Brinkert K, De Causmaecker S, Krieger-Liszkay A, Fantuzzi A, Rutherford AW (2016) Bicarbonate-induced redox tuning in Photosystem II for regulation and protection. Proc Natl Acad Sci USA 113(43):12144–12149. doi:10.1073/pnas.1608862113

Cape JL, Bowman MK, Kramer DM (2006) Computation of the redox and protonation properties of quinones: towards the prediction of redox cycling natural products. Phytochemistry 67(16):1781–1788. doi:10.1016/j.phytochem.2006.06.015

Clarke TA, Edwards MJ, Gates AJ, Hall A, White GF, Bradley J, Reardon CL, Shi L, Beliaev AS, Marshall MJ, Wang Z, Watmough NJ, Fredrickson JK, Zachara JM, Butt JN, Richardson DJ (2011) Structure of a bacterial cell surface decaheme electron conduit. Proc Natl Acad Sci USA 108(23):9384–9389. doi:10.1073/pnas.1017200108

Draper RD, Ingraham LL (1968) A potentiometric study of the flavin semiquinone equilibrium. Arch Biochem Biophys 125:802–808

Frisch MJ, Trucks GW, Schlegel HB, Scuseria GE, Robb MA, Cheeseman JR, Montgomery JA Jr, Vreven T, Kudin KN, Burant JC, Millam JM, Iyengar SS, Tomasi J, Barone V, Mennucci B, Cossi M, Scalmani G, Rega N, Petersson GA, Nakatsuji H, Hada M, Ehara M, Toyota K, Fukuda R, Hasegawa J, Ishida M, Nakajima T, Honda Y, Kitao O, Nakai H, Klene M, Li X, Knox JE, Hratchian HP, Cross JB, Bakken V, Adamo C, Jaramillo J, Gomperts R, Stratmann RE, Yazyev O, Austin AJ, Cammi R, Pomelli C, Ochterski JW, Ayala PY, Morokuma K, Voth GA, Salvador P, Dannenberg JJ, Zakrzewski VG, Dapprich S, Daniels AD, Strain MC, Farkas O, Malick DK, Rabuck AD, Raghavachari K, Foresman JB, Ortiz JV, Cui Q, Baboul AG, Clifford S, Cioslowski J, Stefanov BB, Liu G, Liashenko A, Piskorz P, Komaromi I, Martin RL, Fox DJ, Keith T, Al-Laham MA, Peng CY, Nanayakkara A, Challacombe M, Gill PMW, Johnson B, Chen W, Wong MW, Gonzalez C, Pople JA (2004). Gaussian 03. Gaussian, Inc., Wallingford CT

Hale MB, Blankenship RE, Fuller RC (1983) Menaquinone is the sole quinone in the facultatively aerobic green photosynthetic bacterium *Chloroflexus aurantiacus*. Biochim Biophys Acta 723(3):376–382. doi:10.1016/0005-2728(83)90044-0

Harbury HA, Loach PA (1960) Oxidation-linked proton functions in heme octa- and undecapeptides from mammalian cytochrome *c*. J Biol Chem 235:3640–3645

Hasegawa R, Saito K, Takaoka T, Ishikita H (2017) pK_a of ubiquinone, menaquinone, phylloquinone, plastoquinone, and rhodoquinone in aqueous solution. Photosynth Res 133(1):297–304. doi:10.1007/s11120-017-0382-y

Ishikita H, Knapp E-W (2003) Redox potential of quinones in both electron transfer branches of photosystem I. J Biol Chem 278:52002–52011

Ishikita H, Knapp E-W (2004) Variation of Ser-L223 hydrogen bonding with the Q_B redox state in reaction centers from *Rhodobacter sphaeroides*. J Am Chem Soc 126:8059–8064

Iwaki M, Itoh S (1994) Reaction of reconstituted acceptor quinone and dynamic equilibration of electron transfer in the photosystem I reaction center. Plant Cell Physiol 35:983–993

Jordan P, Fromme P, Witt HT, Klukas O, Saenger W, Krauss N (2001) Three-dimensional structure of cyanobacterial photosystem I at 2.5 Å resolution. Nature 411:909–917

Kato Y, Nagao R, Noguchi T (2016) Redox potential of the terminal quinone electron acceptor Q_B in photosystem II reveals the mechanism of electron transfer regulation. Proc Natl Acad Sci USA 113(3):620–625. doi:10.1073/pnas.1520211113

Kerfeld CA, Sawaya MR, Bottin H, Tran KT, Sugiura M, Cascio D, Desbois A, Yeates TO, Kirilovsky D, Boussac A (2003) Structural and EPR characterization of the soluble form of cytochrome *c*-550 and of the *psbV2* gene product from cyanobacterium *Thermosynechococcus elongatus*. Plant Cell Physiol 44:697–706

Koepp HM, Wendt H, Stkehlow H (1960) Der Vergleich der Spannungsreihen in verschiedenen Solventien. II. Zeitschrift für Elektrochemie. Berichte der Bunsengesellschaft für physikalische Chemie 64 (4):483–491. doi:10.1002/bbpc.19600640406

Li L, Mustafi D, Fu Q, Tereshko V, Chen DL, Tice JD, Ismagilov RF (2006) Nanoliter microfluidic hybrid method for simultaneous screening and optimization validated with crystallization of membrane proteins. Proc Natl Acad Sci USA 103(51):19243–19248. doi:10.1073/pnas.0607502103

Ludwig ML, Pattridge KA, Metzger AL, Dixon MM, Eren M, Feng Y, Swenson RP (1997) Control of oxidation-reduction potentials in flavodoxin from *Clostridium beijerinckii*: the role of conformation changes. Biochemistry 36:1259–1280

Matsui T, Baba T, Kamiya K, Shigeta Y (2012) An accurate density functional theory based estimation of pK_a values of polar residues combined with experimental data: from amino acids to minimal proteins. Phys Chem Chem Phys 14(12):4181–4187

Okamura MY, Paddock ML, Graige MS, Feher G (2000) Proton and electron transfer in bacterial reaction centers. Biochim Biophys Acta 1458:148–163

Prince RC, Dutton PL, Bruce JM (1983) Electrochemistry of ubiquinones: menaquinones and plastoquinones in aprotic solvents. FEBS Lett 160:273–276

Ptushenko VV, Cherepanov DA, Krishtalik LI, Semenov AY (2008) Semi-continuum electrostatic calculations of redox potentials in photosystem I. Photosynth Res 97(1):55–74. doi:10.1007/s11120-008-9309-y

Rabenstein B, Ullmann GM, Knapp E-W (1998) Energetics of electron-transfer and protonation reactions of the quinones in the photosynthetic reaction center of *Rhodopseudomonas viridis*. Biochemistry 37:2488–2495

Robinson HH, Crofts AR (1984) Kinetics of proton uptake and the oxidation-reduction reactions of the quinone acceptor complex of photosystem II from pea chloroplasts. In: Sybesma C (ed) Advances in photosynthesis research, vol 1. Martinus Nijhoff/Dr. W. Junk Publishers, The Hague, pp 477–480

Rutherford AW, Renger G, Koike H, Inoue Y (1984) Thermoluminescence as a probe of photosystem II. The redox and protonation states of the secondary acceptor quinone and the O_2-evolving enzyme. Biochim Biophys Acta 767(3):548–556

Saito K, Shen J-R, Ishida T, Ishikita H (2011) Short hydrogen-bond between redox-active tyrosine Y_Z and D1-His190 in the photosystem II crystal structure. Biochemistry 50:9836–9844

Sakashita N, Watanabe HC, Ikeda T, Saito K, Ishikita H (2017) Origins of water molecules in the photosystem II crystal structure. Biochemistry 56(24):3049–3057. doi:10.1021/acs.biochem.7b00220

Schmidt am Busch M, Knapp E-W (2005) One-electron reduction potential for oxygen- and sulfur-centered organic radicals in protic and aprotic solvents. J Am Chem Soc 127:15730–15737

Swallow AJ (1982) Physical chemistry of semiquinones. In: Trumpower BL (ed) Function of quinones in energy conserving systems. Academic Press, New York, pp 59–72

Taguchi AT, Mattis AJ, O'Malley PJ, Dikanov SA, Wraight CA (2013) Tuning cofactor redox potentials: the 2-methoxy dihedral angle generates a redox potential difference of >160 mV between the primary (Q_A) and secondary (Q_B) quinones of the bacterial photosynthetic reaction center. Biochemistry 52(41):7164–7166. doi:10.1021/bi4011896

Takaoka T, Sakashita N, Saito K, Ishikita H (2016) pK_a of a proton-conducting water chain in photosystem II. J Phys Chem Lett 7:1925–1932. doi:10.1021/acs.jpclett.6b00656

Umena Y, Kawakami K, Shen J-R, Kamiya N (2011) Crystal structure of oxygen-evolving photosystem II at a resolution of 1.9 Å. Nature 473:55–60

Vos MH, van Gorkom HJ (1990) Thermodynamical and structural information on photosynthetic systems obtained from electroluminescence kinetics. Biophys J 58(6):1547–1555. doi:10.1016/S0006-3495(90)82499-1

Watanabe T, Kobayashi M (1991) Electrochemistry of chlorophylls. In: Scheer H (ed) Chlorophylls. CRC Press, Boca Raton, pp 287–303

Watt W, Tulinsky A, Swenson RP, Watenpaugh KD (1991) Comparison of the crystal structures of a flavodoxin in its three oxidation states at cryogenic temperatures. J Mol Biol 218:195–208

Wilson GS (1983) Electrochemical studies of porphyrin redox reactions as cytochrome models. Bioelectrochem Bioenerg 1:172–179

Wraight CA (2004) Proton and electron transfer in the acceptor quinone complex of photosynthetic reaction centers from *Rhodobacter sphaeroides*. Front Biosci 9:309–337

Zhu Z, Gunner MR (2005) Energetics of quinone-dependent electron and proton transfers in *Rhodobacter sphaeroides* photosynthetic reaction centers. Biochemistry 44:82–96